J|A|C|S
ARTICLES
Published on Web 03/01/2003

Supramolecular Pseudorotaxane Polymers from Complementary Pairs of Homoditopic Molecules

Harry W. Gibson,* Nori Yamaguchi, and Jason W. Jones

Contribution from the Department of Chemistry, Virginia Tech, Blacksburg, Virginia 24061

Received July 1, 2002; E-mail: hwgibson@vt.edu

Abstract: Self-assembly of supramolecular pseudorotaxane polymers from complementary homoditopic building blocks comprised of bis(dibenzo-24-crown-8) esters derived from the hydroxymethyl crown ether and aliphatic diacid chlorides (**CxC**, x = number of methylene units in the diacid segment) and 1,10-bis-[*p*-(benzylammoniomethyl)phenoxy]alkane bis(hexafluorophosphate)s (**AyA**, y = number of methylene units in the linker) has been studied. ^{1}H NMR spectroscopic studies of bis[(2-dibenzo-24-crown-8)methyl] sebacate (**C8C**) with dibenzylammonium hexafluorophosphate (**6**) showed that the two binding sites of the ditopic host are equivalent and independent (no positive or negative cooperativity). Likewise the binding sites in 1,10-bis[*p*-(benzylammoniomethyl)phenoxy]decane bis(hexafluorophosphate) (**A10A**) were shown to behave independently with dibenzo-24-crown-8 (**1a**). Then using ^{1}H NMR spectroscopy on dilute equimolar solutions (<1 mM) of **CxC** and **AyA** association constants were estimated for the formation of the linear (***lin*-CxC•AyA**) and cyclic (***cyc*-CxC•AyA**) dimers, thus enabling effective molarities to be estimated for the various systems. Finally ^{1}H NMR spectroscopy was used to semiquantitatively or qualitatively demonstrate the formation of linear supramolecular polymers ***lin*-[CxC•AyA]$_n$** in more concentrated solutions (up to 2.0 M) of the complementary pairs of **CxC** and **AyA**. The sizes of the assemblies (*n* values) are not as great as the dilute solution studies predict; this is attributed to the deleterious effect of ionic strength and exo complexation at high concentrations. However, as expected from the dilute solution results, linear extension is indeed favored with the longer building blocks, meaning that "monomer" end-to-end distance is a key factor in reducing the amount of cyclic species that form. Viscosity experiments clearly demonstrate the formation of large noncovalent polymers ***lin*-[CxC•AyA]$_n$** in concentrated solutions. Cohesive film and fiber formation also indicate that supramolecular polymers of sufficient size to enable entanglement self-assemble in these solutions.

Introduction

Chemists are extending the concept of self-organizing noncovalent interactions from supramolecular science[1] into the field of material science to produce novel structures with functional properties. The formation of noncovalently bound crystalline, "polymeric" solids has a long history,[2] but much progress has been made recently.[3]

The self-assembly and study of "noncovalent polymers" in solution is more recent; the aims are to control and engineer linear and network supramolecular polymers using the liquid phase to facilitate the process and ultimately produce films or fibers. Such interactions permit reversibility at the molecular level, affording thermodynamically controlled polymeric suprastructures. This is advantageous from the point of view of producing polymers with potential for commercial use, since kinetically induced defects in conventional covalently bonded polymers are irreversible. Indeed, it has been shown that strong associations between self-organizing building blocks promote the construction of well-defined supramolecular polymeric materials with properties comparable to covalent polymers.[4]

(1) Vögtle, F. *Supramolecular Chemistry*; John Wiley and Sons: New York, 1991. Cram, D. J.; Cram, J. M. *Container Molecules and Their Guests*; Royal Society of Chemistry, Cambridge, UK, 1994. Lehn, J.-M. *Supramolecular Chemistry*; VCH Publishers: New York, 1995. *Comprehensive Supramolecular Chemistry*; Atwood, J. L., Davies, J. E. D., MacNicol, D. D., Vögtle, F., exec. Eds.; Pergamon Press: New York, 1996. Moore, J. S. *Curr. Opin. Colloid Interfac. Sci.* **1999**, *4*, 108−116. Caulder, D. L.; Raymond, K. N. *Acc. Chem. Res.* **1999**, *32*, 975−982. Rowan, A. E.; Elemans, J. A. A. W.; Nolte, R. J. M. *Acc. Chem. Res.* **1999**, *32*, 995−1006. Leininger, S.; Olenyuk, B.; Stang, P. J. *Chem. Rev.* **2000**, *100*, 853−908. Lindoy, L. F.; Atkinson, I. M. *Self-Assembly in Supramolecular Systems*; Royal Society of Chemistry: Cambridge, UK, 2000. Steed, J. W.; Atwood, J. L. *Supramolecular Chemistry*; J. Wiley and Sons: New York, 2000. Holliday, B. J.; Mirkin, C. A. *Angew. Chem., Int. Ed.* **2001**, *40*, 2022−2043.

(2) Schmidt, G. J. *Pure Appl. Chem.* **1971**, *27*, 647−678.

(3) Inter alia: Desiraju, G. R. *Acc. Chem. Res.* **1996**, *29*, 441−449. Karle, I. L.; Ranganathan, D.; Haridas, V. *J. Am. Chem. Soc.* **1997**, *119*, 2777−2783. Brunet, P.; Simard, M.; Wuest, J. D. *J. Am. Chem. Soc.* **1997**, *119*, 9, 2737−2738. Hajek, F.; Hosseini, M. W.; Graf, E.; De Cian, A.; Fischer, J. *Angew. Chem., Int. Ed. Engl.* **1997**, *36*, 1760−1762. Desiraju, G. R. *Chem. Rev.* **1998**, *98*, 1375−1406. Batten, S. R.; Robson, R. *Angew. Chem., Int. Ed.* **1998**, *37*, 1461−1494. Marsman, A. W.; Leussink, E. D.; Zwikker, J. W.; Jenneskens, L. W. *Chem. Mater.* **1999**, *11*, 1484−1491. Ozin, G. A. *Chem. Commun.* **2000**, 419−432. Moulton, B.; Zaworotko, M. J. *Chem. Rev.* **2001**, *101*, 1629−1658. Holman, K. T.; Pivovar, A. M.; Swift, J. A.; Ward; M. D. *Acc. Chem. Res.* **2001**, *34*, 107−118. Ward, M. D. *Chem. Rev.* **2001**, *101*, 1697−1726. Nguyen, T. L.; Fowler, F. W.; Lauher, J. W. *J. Am. Chem. Soc.* **2001**, *123*, 11057−11064.

(4) H-bonded systems: Lehn, J.-M. *Makromol. Chem., Macromol. Symp.* **1993**, *69*, 1−17. Rebek, J., Jr. *Chem. Commun.* **2000**, 637−643. Kato, T.; Mizoshita, N.; Kanie, K. *Macromol. Rapid Commun.***2001**, *22*, 797−814. Meijer E. W.; Brunsveld, L.; Folmer, B. J. B.; Meijer, E. W.; Sijbesma, R. P. *Chem. Rev.* **2001**, *101*, 4071−4098. Berl, V.; Schmutz, M.; Krische, M. J.; Khoury, R. G.; Lehn, J.-M. *Chem. Eur. J.* **2002**, *8*, 1227−1244. Metal-induced systems: Schubert, U. S.; Hien, O.; Eschbaumer, C. *Macromol. Rapid Commun.* **2000**, *21*, 1156−1161.

10.1021/ja020900a CCC: $25.00

Scheme 1. Syntheses of Homoditopic Hosts, Bis(dibenzo-24-crown-8) Esters **C8C** and **C2C**, and Bis(*m*-phenylene)-26-crown-8 Ester **MC8MC**

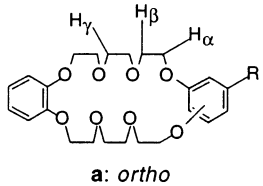

a: *ortho*
b: *meta*

1. R = H
2. R = CH_2OH
7. R = $COOCH_3$

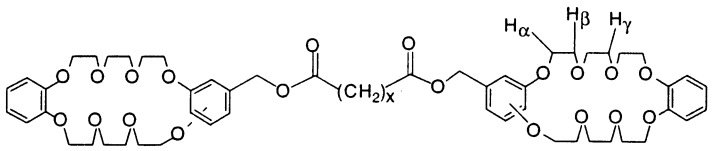

C8C. x = 8, *ortho, ortho*
C2C. x = 2, *ortho, ortho*
MC8MC. x = 8, *meta, meta*

Pseudorotaxanes, in which linear molecules are threaded through cyclic species, have been intensely investigated over the past decade.[5] There have been several reports of attempts to use this structural motif to self-assemble noncovalent polymers,[6] including preliminary accounts from this laboratory.[7] In one of our efforts we utilized a relatively simple system with dibenzylammonium hexafluorophosphate guest and dibenzo-24-crown-8 (DB24C8) host units in a pair of homoditopic building blocks.[7a] For the model monotopic building blocks the association constant for pseudorotaxane formation is reported to be desirably high ($K_a = 2.7 \times 10^4$ M^{-1} in chloroform-*d* at 25 °C).[8] Association of homoditopic molecules containing such complementary units spontaneously leads to reversible chain extension in 1:1 stoichiometric solutions, forming linear supramolecular polymers based on pseudorotaxane formation, as we describe in this work.

Our approach seeks to incorporate flexible units into both building blocks for two reasons: (1) to increase solubility, particularly in the nonpolar solvents required for these complexations, enabling the necessary high concentrations to be achieved and (2) to produce amorphous or semicrystalline supramolecular polymers having better mechanical properties than fully crystalline solids.

Results and Discussion

I. Synthesis of Building Blocks. The synthetic methodologies employed for the homoditopic host molecules are depicted in Scheme 1. The primary alcohols **2**[7a] were esterified to afford the homoditopic hosts, bis(crown ether)s **C2C**, **C8C**,[7a] and **MC8MC**.[7a]

Syntheses of homoditopic guests 1,10-bis[*p*-(benzylammoniomethyl)phenoxy]alkane bis(hexafluorophosphate)s, diammonium salts (**AyA**), are shown in Scheme 2. The PF_6^- salts showed improved solubility in organic solvents such as acetone and acetonitrile compared to Cl^- salts. The lack of solubility of the salts **A4A**, **A10A**, and **A22A** in $CDCl_3$ precluded use of this solvent for complexation studies; however, all the precursors are soluble in acetone-d_6 and 1:1 acetone-d_6:$CDCl_3$.

II. Model Complexation Studies. Since both the host and guest species are ditopic, the possibility exists in each case that the binding is statistical, positively cooperative, or anticooperative.[9] In these model studies the binding of complementary monotopic complementary species was examined to determine which situation obtained.

II. a. Ditopic Guest A10A and Monotopic Host Dibenzo-24-crown-8 (1a). The C_{10}-linked diammonium salt **A10A** was examined with DB24C8 (**1a**) at 22 °C in acetone-d_6 by ^{1}H NMR spectroscopy. The concentration of **A10A** was held constant at 10 mM, and the crown concentration was systematically varied. The extent of complexation, *p*, of the ammonium moieties to form pseudorotaxanes was determined by integration of (1) the NCH_2 signals for complexed (4.77 and 4.67 ppm) versus uncomplexed (4.60 and 4.58 ppm) species and (2) the signal for H_{yc} in the complex (d, 6.70 ppm) versus H_{yu} in the uncomplexed state (d, 6.99 ppm) observed under slow exchange.[10] The results are shown in Figure 1a in the form of a Scatchard plot.[9] The linear nature of the plot indicates that the two binding sites of **A10A** are independent of each other and that they behave in a noncooperative mode.[9] The association constants[11] K_1 and K_2 (see Scheme 3a) for formation of the [2]- and [3]-pseudorotaxanes, therefore, will be in the ratio 2:0.5, based on statistics.[9] The negative of the slope of the Scatchard plot is the average of K_1 and K_2 and the intercept is K_{ave}. Taking the average of the slope and intercept values [1.4 (±0.1) ×

(5) For reviews of pseudorotaxanes and rotaxanes, see: Amabilino, D. B.; Stoddart, J. F. *Chem. Rev.* **1995**, *95*, 2725−2828. Gibson, H. W. in *Large Ring Molecules*; Semlyen, J. A., Ed.; John Wiley and Sons: New York, 1996; Chapter 6, pp 191−262. Nepogodiev, S. A.; Stoddart, J. F. *Chem. Rev.* **1998**, *98*, 1959−1976. Raymo, F. M.; Stoddart, J. F. *Chem. Rev.* **1999**, *99*, 1643−1664. Sauvage, J.-P., Dietrich-Buchecker, C. O., Eds. *Molecular Catenanes, Rotaxanes and Knots*; Wiley-VCH: Weinheim, 1999. Hubin, T. J.; Busch, D. H. *Coord. Chem. Rev.* **2000**, *200*−*202*, 5−52. Cantrill, S. J.; Pease, A. R.; Stoddart, J. F. *J. Chem. Soc., Daltons Trans.* **2000**, 3715−3734. Mahan, E.; Gibson, H. W. in *Cyclic Polymers*, 2nd ed.; Semlyen, J. A., Ed.; Kluwer Publishers: Dordrecht, 2000; pp 415−560.

(6) Hirotsu, K.; Higuchi, T.; Fujita, K.; Ueda, T.; Shinoda, A.; Imoto, T.; Tabushi, I. *J. Org. Chem.* **1982**, *47*, 1143−1144. Alvarez-Parrilla, E.; Cabrer, P. R.; Al-Soufi, W.; Meijide, F.; Nunez, E. R.; Tato, J. V. *Angew. Chem., Int. Ed.* **2000**, *39*, 2856−2858. Sandier, A.; Brown, W.; Mays, H.; Amiel, C. *Langmuir* **2000**, *16*, 1634−1642. Hoshino, T.; Miyauchi, M.; Kawaguchi, Y.; Yamaguchi, H.; Harada, A. *J. Am. Chem. Soc.* **2000**, *122*, 9876−9877. Cantrill, S. J.; Youn, G. J.; Stoddart, J. F. *J. Org. Chem.* **2001**, *66*, 6857−6872.

(7) (a) Yamaguchi, N.; Gibson, H. W. *Angew. Chem., Int. Ed.* **1999**, *38*, 143−147. (b) Yamaguchi, N.; Gibson, H. W. *Chem. Commun.***1999**, 789−790. (c) Yamaguchi, N.; Nagvekar, D. S.; Gibson, H. W. *Angew. Chem., Int. Ed.* **1998**, *37*, 2361−2364.

(8) Ashton, P. R.; Campbell, P. J.; Chrystal, E. J. T.; Glink, P. T.; Menzer, S.; Philp, D.; Spencer, N.; Stoddart, J. F.; Tasker, P. A.; Williams, D. J. *Angew. Chem. Int. Ed. Engl.* **1995**, *34*, 1865−1869. Ashton, P. R.; Chrystal, E. J. T.; Glink, P. T.; Menzer, S.; Schiavo, C.; Spencer, N.; Stoddart, J. F.; Tasker, P. A.; White, A. J. P.; Williams, D. J. *Chem. Eur. J.* **1996**, *2*, 709−728. Fyfe, M. C. T.; Stoddart, J. F. *Adv. Supramol. Chem.* **1999**, *5*, 1−53. Chang, T.; Heiss, A. M.; Cantrill, S. J.; Fyfe, M. C. T.; Pease, A. R.; Rowan, S. J.; Stoddart, J. F.; Williams *Org. Lett.* **2000**, *2*, 2943−2946. Chang, T.; Heiss, A. M.; Cantrill, S. J.; Fyfe, M. C. T.; Pease, A. R.; Rowan, S. J.; Stoddart, J. F.; White, A. J. P.; Williams, D. J. *Org. Lett.* **2000**, *2*, 2947−2950. Cantrill, S. J.; Pease, A. R.; Stoddart, J. F. *J. Chem. Soc., Dalton Trans.* **2000**, 3715−3734. Amirsakis, D. G.; Garcia-Garibay, M. A.; Rowan, S. J.; Stoddart, J. F.; White, A. J. P.; Williams, D. J. *Angew. Chem., Int. Ed.* **2001**, *40*, 4256−4261.

(9) Freifelder, D. M. *Physical Biochemistry*; W. H. Freeman and Co.: New York, 1982; pp 659−660. Marshall, A. G. *Biophysical Chemistry*; J. Wiley and Sons: New York, 1978; pp 70−77. Connors, K. A. *Binding Constants*; J. Wiley and Sons: New York, 1987; pp 78−86.

(10) See Supporting Information.

(11) Association constants reported here are based on K_a = [pseudorotaxane]/([crown]$_o$ − [pseudorotaxane])([ammonium salt]$_o$ − [pseudorotaxane]); that is, they are concentration-based and assume that all nonpseudorotaxane species are "free". This is the usual method of calculating such association constants; see ref 5.

Scheme 2. Syntheses of Homoditopic Guests: Diammonium Salts **AyA**, y = Number of Methylene or Ethyleneoxy (EO) Units in the Spacer R[a]

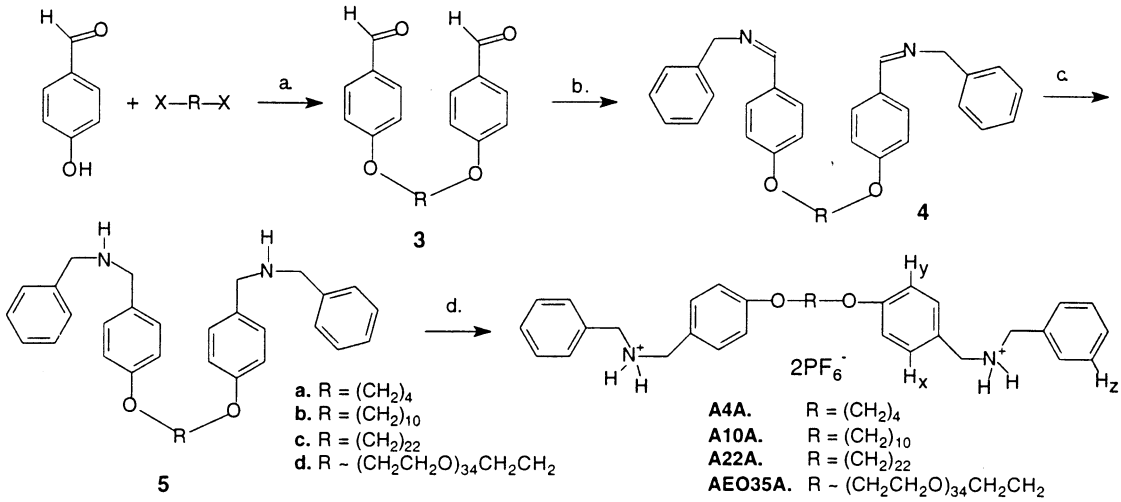

[a] Reaction conditions: a. K_2CO_3/DMF/110 °C. b. $C_6H_5CH_2NH_2$/toluene/110 °C. c. $NaBH_4$/MeOH, 25 °C. d. 1) HCl, 2) NH_4PF_6.

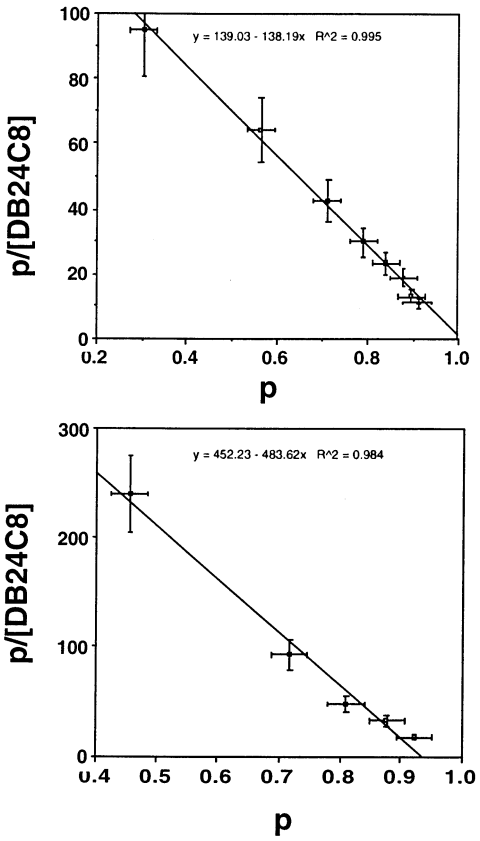

Figure 1. Scatchard plots derived from ^{1}H NMR data for complexation of homoditopic guest **A1A0** (total concentration 10 mM) with monotopic host dibenzo-24-crown-8 (**1a**) (total concentration varied from 10 mM to 0.10 M): (a) (top) in acetone-d_6 and (b) (bottom) in acetone-d_6:choroform-*d* (1:1, v:v). p = fraction of ammonium moieties bound. p was determined from integration of the signals for uncomplexed and complexed NCH_2 at 4.68/4.77 and 4.56/4.59 ppm in (a), and 4.40 and 4.54/4.64 ppm in (b), respectively. These values in (b) were confirmed using the signal for complexed H_y at 6.62 ppm versus the signal for uncomplexed H_z at 7.46 ppm. [**1a**] was determined from the percentage of uncomplexed **A10A**. Error bars in p: ±0.03 absolute; error bars in p/[DB24C8]: ±15% relative.

10^2 M^{-1}] from the Scatchard plot, K_1 was determined to be 2.2 (±0.1) × 10^2 M^{-1} and K_2 = 55 ± 1 M^{-1}. This system was similarly examined in acetone-d_6/chloroform-*d* (1/1, v/v) using (1) NCH_2 signals in the complexed (4.54 and 4.64 ppm) and

Scheme 3. Sequential Formation of [2]- and [3]Pseudorotaxanes from (a) (left) a Homoditopic Guest and a Monotopic Host and (b) (right) a Homoditopic Host and a Monotopic Guest

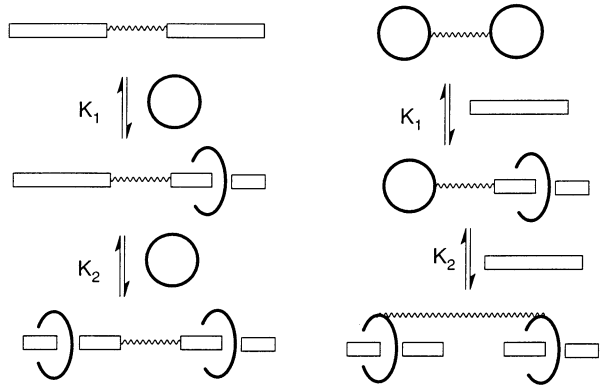

uncomplexed (~4.4 ppm) states and (2) H_{yc} complexed (d, 6.63 ppm) versus H_{xu} uncomplexed (m, 7.46 ppm). Again the linear Scatchard plot (Figure 1b) confirmed the independent, noncooperative nature of the two complexation sites of **A10A**. In this solvent system from K_{ave} [4.7 (±0.2) × 10^2 M^{-1}], K_1 = 7.5 (±0.3) × 10^2 M^{-1} and K_2 = 1.9 (±0.1) × 10^2 M^{-1}. The average values from the Scatchard plots may be compared with association constants[11] of 2.0 (±0.1) × 10^2 M^{-1} and 4.6 (±0.1) × 10^2 M^{-1} determined by us for the monotopic system dibenzylammonium hexafluorophosphate (**6**) (10 mM) /DB24C8 (**1a**) (concentration varied from 10 to 30 mM) in acetone-d_6 and acetone-d_6:chloroform-*d* (1:1, v:v), respectively. The agreement for the two systems in the mixed solvent is within experimental error, as expected[9] if the ammonium sites in **A10A** are essentially equivalent to that in dibenzylammonium hexafluorophosphate (**6**).

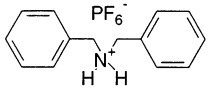

6

II. b. Ditopic Guest AEO35A and Monotopic Dibenzo-24-crown-8 (1a). The ^{1}H NMR spectra of a series of chloroform-*d* solutions of **AEO35A** and DB24C8 (**1a**) (10/10−10/40

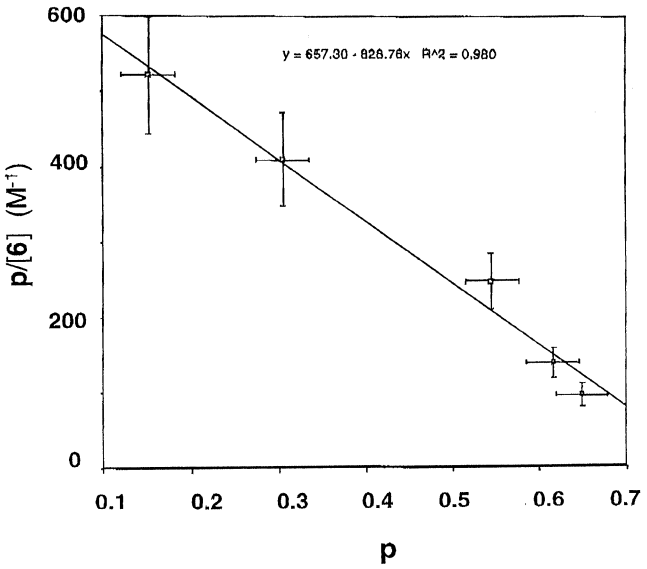

Figure 2. Scatchard plot derived from ^{1}H NMR data for complexation of homoditopic host **C8C** (total concentration 2.46 mM) with monotopic guest dibenzylammonium hexafluorophosphate (**6**) (total concentration varied from 1.20 to 15.0 mM) in acetone-d_6:choroform-*d* (1:1, v:v). p = fraction of crown ether moieties bound. p was determined from integration of the signals for uncomplexed and complexed γ-protons at 3.73 and 3.49 ppm, respectively; [**6**] was determined by integration of the signals for uncomplexed and complexed NCH_2 signals at 4.46 and 4.65 ppm, respectively. Error bars in p: ±0.03 absolute; error bars in p/[DB24C8]: ±15% relative.

mM at 22 °C) were recorded to study the binding affinity of **AEO35A**. From the linear Scatchard plot the average apparent association constant[11] for pseudorotaxane formation (K_{ave}) was determined to be 20 ± 3 M^{-1}, yielding $K_1 = 32 \pm 5$ M^{-1} and $K_2 = 8 \pm 1$ M^{-1}. The 1000-fold lower apparent K_a value obtained relative to the model system composed of dibenzylammonium hexafluorophosphate (**6**) and DB24C8 (**1a**) [2.7 × 10^4 M^{-1} in $CDCl_3$ at 25 °C][8] is undoubtedly a consequence of competitive intra- and intermolecular hydrogen bonding between the 34 aliphatic oxygen atoms of the PEO linker segment and ammonium salt moieties of **AEO35A**, reducing the true concentration of the latter species in the free state. The same effect was noted for solutions in $CDCl_3$:acetone-d_6 (1:1, v:v) [$K_1 = 40 \pm 8$ M^{-1}, $K_2 = 10 \pm 2$ M^{-1} at 22°C].[11]

II. c. Ditopic Host C8C with Monotopic Guest Dibenzylammonium Hexafluorophosphate (6). The interaction of **C8C** with dibenzylammonium hexafluorophosphate (**6**) to form [2]- and [3]pseudorotaxanes (Scheme 3b) was also studied. The concentration of **C8C** was maintained at 2.46 mM and that of **6** was varied from 1 to 15 mM in acetone-d_6/chloroform-*d* (1/1, v/v). Extents of complexation were determined by ^{1}H NMR by comparison of integrals for complexed (3.48 ppm) vs uncomplexed (3.72 ppm) γ-protons.[10] As can be seen in Figure 2 the Scatchard plot is linear, meaning that the two host sites in **C8C** act independently and equivalently. [9] From the values of the slope and intercept the average apparent association constant[11] for pseudorotaxane formation (K_{ave}) was determined to be 7.4 (±0.6) × 10^2 M^{-1}, yielding $K_1 = 1.2$ (±0.1) × 10^3 M^{-1} and $K_2 = 3.0$ (±0.2) × 10^2 M^{-1}. These values are higher than those for the model system consisting of dibenzo-24-crown-8 (**1a**) and homoditopic guest **A10A** [$K_1 = 7.5$ (±0.3) × 10^2 M^{-1} and $K_2 = 1.9$ (±0.1) × 10^2 M^{-1}] and K_{ave} is greater than K_a for **1a•6** [4.6 (±0.1) × 10^2 M^{-1}] under similar conditions. The differences are attributed to substituent effects.[12] Diammonium salt **A10A** has an electron-donating alkoxy group para to the NCH_2 moiety; this is expected to decrease the acidity of **A10A** relative to dibenzylammonium hexafluorophosphate (**6**). On the other hand bis(crown ether) **C8C** possesses a CH_2-OOC moiety that may increase its basicity relative to dibenzo-24-crown-8 (**1a**). [No Hammett constants could be found for this substituent.] Thus, the pair **C8C**/**6** consists of the more active host and guest species relative to both **1a**/**A10A** and **1a**/**6**.

III. Complexation Studies in Dilute Solutions: Dependence of Cyclization on Spacer Length. The formation of cyclic species[14] is a competitive pathway that detracts from the formation of high molar mass linear supermolecules. Therefore, we next investigated the relative stabilities of cyclic and linear dimeric complexes **cyc-CxC•AyA** and **lin-CxC•AyA**, respectively, (Scheme 4) based on homoditopic guest molecules **A4A** through **A22A** and host **C8C**.

To identify and assign ^{1}H NMR signals for these species, a series of 10 mM solutions of **A10A** was prepared using nonstoichiometric amounts of **C8C** (from 20 to 80 mM), and the ^{1}H NMR spectra were recorded (Figure 3). Increasing the concentration of **C8C** with respect to **A10A** shifts the complexation equilibrium toward the 1:2 complex ***lin*-C8C•-A10A•C8C**, analogous to the [3]pseudorotaxane of Scheme 3a, emulating the environment of the internal, i.e., complexed, benzylic *N*-methylene units in linear dimer **lin-C8C•A10A** and extended ***lin*-[C8C•A10A]$_n$**. Since the signals at 4.53 and 4.63 ppm became more intense as [**C8C**] increased while the signals at 4.45 and 4.74 ppm became less intense, the former (inner) signals correspond to the linearly linked chains ***lin*-[C8C•A10A]$_n$**, ***lin*-[C8C•A10A]$_n$•C8C** and ***lin*-[A10A•C8C]$_n$•A10A**), and the latter (outer) signals, to the cyclic dimer **cyc-C8C•A10A**. The integral ratio of the outer to the inner signals decreased from 3.4 at 10/10 mM to 0.29 at 10/80 mM. The chemical shifts of the complexed NCH_2 signals for the linearly linked species ***lin*-C8C•A10A** and ***lin*-[C8C•A10A]$_n$** are consistent with the positions of analogous signals in the model [2]pseudorotaxane from DB24C8 (**1a**) and ditopic guest **A10A**, 4.54 and 4.64 ppm, as described above. Signals in the aromatic region were used for corroboration. The signal for H_{yu} of the diammonium component of the cyclic dimer ***cyc*-C8C•A10A** appears upfield (6.49 ppm) relative to complexed H_{yc} of linear species ***lin*-[A10A•C8C]$_n$•A10A** (6.64 ppm); note that the latter is essentially the same position as analogous signals in **1a•A10A** (6.63 ppm, see above). Likewise complexed H_{xc} of cyclic dimer ***cyc*-C8C•A10A** at 7.00 ppm (a doublet) was distinct over most of the concentration range examined.

To evaluate quantitatively the equilibria leading to ***cyc*-CxC•AyA** and ***lin*-CxC•AyA** it is necessary to use concentrations that do not allow the formation of higher linear oligomers.

(12) Substituent effects for secondary ammonium salts in complexation with DB24C8 follow the Hammett equation: Ashton, P. R.; Fyfe, M. C. T.; Hickingbottom, S. K.; Stoddart, J. F.; White, A. J. P.; Williams, D. J. *J. Chem. Soc., Perkin Trans. 2* **1998**, 2117−2128. We have shown that the electron-withdrawing carbomethoxy substituent on the crown ether in the pair **6**/**7a** causes a lower K_a than observed with **1a**/**6** (ref 13).

(13) Gibson, H. W.; Yamaguchi, N.; Hamilton, L.; Jones, J. W. *J. Am. Chem. Soc.* **2002**, *124*, 4653−4665.

(14) Cyclic dimer formation in other ditopic pseudorotaxane systems: Ashton, P. R.; Baxter, I.; Cantrill, S. J.; Fyfe, M. C. T.; Glink, P. T.; Stoddart, J. F.; White, A. J. P.; Williams, D. J. *Angew. Chem., Int. Ed.* **1998**, *37*, 1294−1297. Cyclic dimers in quadruple hydrogen bonded systems: Söntjens, S. H. M.; Sijbesma, R. P.; van Genderen, M. H. P.; Meijer, E. W. *Macromolecules* **2001**, *34*, 3815−3818.

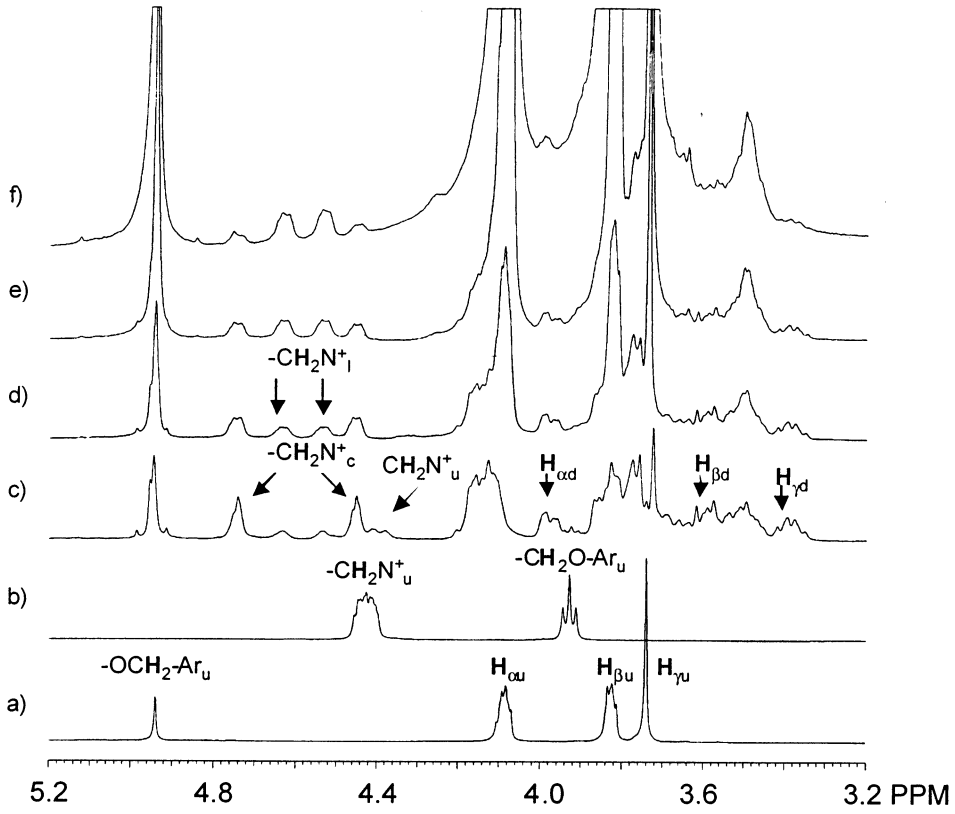

Figure 3. ^{1}H NMR spectra of solutions of **C8C** and **A10A** at (a) 10/0, (b) 0/10, (c) 10/10, (d) 20/10, (e) 40/10, (f) 80/10 mM/mM (400 MHz, acetone-d_6:chloroform-*d* (1:1, v:v), 22 °C). The three sets of NCH_2 signals are for (1) uncomplexed moieties, i.e., end groups, (denoted by "u") in **A10A**, ***lin*-[A10A•C8C]$_n$•A10A** and ***lin*-[C8C•A10A]$_n$**, (2) complexed moieties (denoted by "l") in ***lin*-[C8C•A10A]$_n$**, ***lin*-[A10A•C8C]$_n$•A10A** and ***lin*-[C8C•A10A]$_n$•C8C**, and 3) complexed moieties in ***cyc*-C8C•A10A** (denoted by "c"). As the proportion of **C8C** increases statistics predict that ***lin*-[C8C•A4A]$_n$•C8C**, $n = 1$ will become the predominant species.

Scheme 4. Cartoon Illustration of Construction of Linear and Cyclic Dimers ***lin*-CxC•AyA** and ***cyc*-CxC•AyA**, and Supramolecular Assemblies ***lin*-[CxC•AyA]$_n$**, ***lin*-[CxC•AyA]$_n$•CxC** and ***lin*-[AyA•CxC]$_n$•AyA**

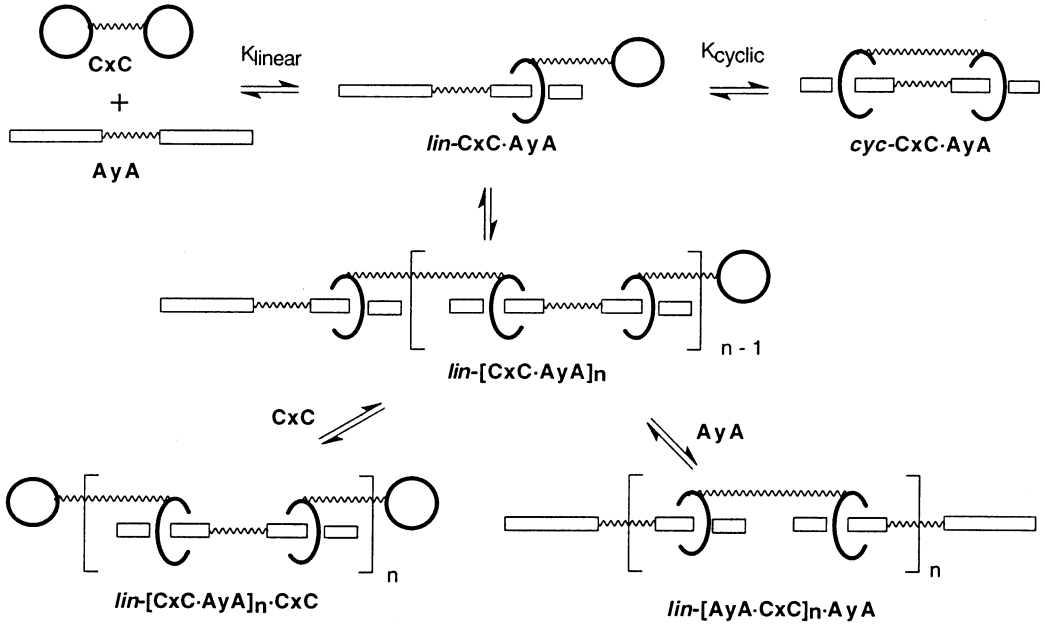

Therefore, the ^{1}H NMR spectra of quite dilute (0.2 and 0.4 mM) equimolar solutions of **C8C** individually with **A4A** through **A22A** were examined. These revealed four sets of $N-CH_2$ signals (Figure 4a−c) corresponding to (1) uncomplexed moieties of the ditopic guest molecule **AyA** (∼4.3 ppm), (2) complexed moieties in cyclic dimer ***cyc*-CxC•AyA** (∼4.45 and 4.75 ppm), (3) complexed (∼4.55 and 4.65 ppm) and (4) uncomplexed (∼4.4 ppm) moieties in the linear dimer **lin-CxC•AyA**, respectively. Figure 4d for the model system from DB24C8 (**1a**) and **A10A** displays signals for the benzylic protons of the ammonium salt units in **A10A** (totally uncomplexed, u) and the [2]pseudorotaxane ***lin*-C8C•A10A** (com-

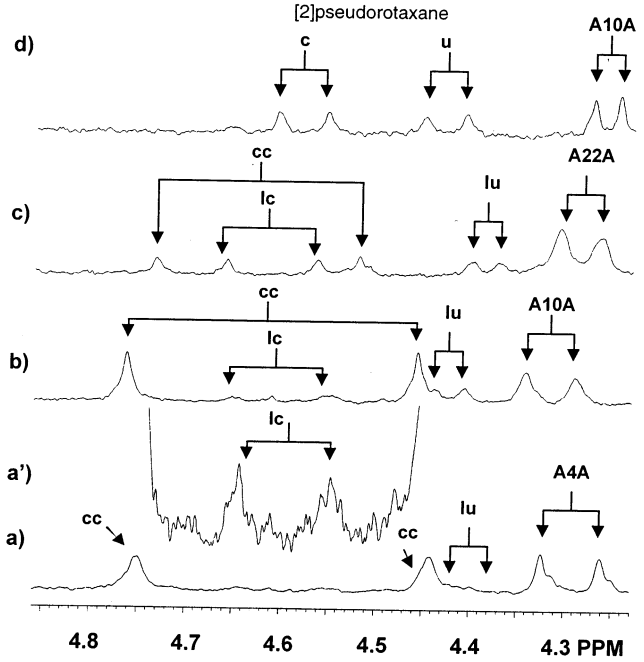

Figure 4. Partial ^{1}H NMR spectra (NCH_2 region) of equimolar solutions of (a) **C8C** and **A4A**, (b) **C8C** and **A10A**, and (c) **C8C** and **A22A** (0.40 mM each), and (d) a solution of DB24C8 (**1a**) and **A10A** (0.80/0.40 mM) at 22 °C (400 MHz, acetone-d_6:chloroform-*d*, 1:1, v:v). The four pairs of NCH_2 signals in (a−c) are for (1) uncomplexed moieties in **AyA**, (2) uncomplexed moieties (end groups) of linear dimers ***lin*-C8C•AyA**, denoted by "lu", (3) complexed moieties in ***lin*-C8C•AyA**, (denoted by "lc") and complexed moieties in ***cyc*-C8C•AyA** (denoted by "cc"). In (d) the upfield pair of signals is for the NCH_2 protons of **A10A**; the next downfield pair of signals is for the uncomplexed NCH_2 protons of the [2]pseudorotaxane, denoted by "u", and the most downfield pair derives from the complexed NCH_2 protons of the pseudorotaxane, denoted by "c".

plexed end = c, and uncomplexed end = u). An expanded version of the spectrum in Figure 4a in the region of 4.45−4.75 ppm is shown in Figure 4a′. The ^{1}H NMR spectra of three sets of each pair (0.20 and 0.40 mM each) were recorded with at least 50 min of acquisition time and integrated using a deconvolution technique.

The ratios of each uncomplexed/complexed pair of signals for ***lin*-CxC•AyA** was determined to be 1:1 (±5%), confirming that they arise from this species and not from higher oligomers which would yield ratios of <1:1. These spectroscopic observations allowed us to conclude that only ***lin*-CxC•AyA** and ***cyc*-CxC•AyA** exist; larger cyclic[15] and linear oligomers ***lin*-[CxC•AyA]$_n$**, $n > 1$ are not present in detectable amounts in these dilute solutions. Since the concentrations of each species (**CxC**, **AyA**, ***lin*-CxC•AyA**, and ***cyc*-CxC•AyA**) at equilibrium are known, one can estimate the association constants K_{linear} and K_{cyclic} (see Scheme 4).[11] K_{linear} (Table 1) varies systematically, increasing as the length of the aliphatic spacer increases (from **A4A** to **A22A**). Similarly, K_{cyclic} varies systematically, decreasing as the length of the aliphatic spacer increases (from **A4A** to **A22A**). With increasing spacer length y, ΔG_{linear} becomes more negative and ΔG_{cyclic} becomes more positive (Figure 5a). These observations are consistent with the importance of the increasing penalty for cyclization as the end-to-end distance increases.[16,17] As we anticipated, K_{cyclic} for **C8C•A22A** was reduced, 4-fold, compared to that for **C8C•A4A**. Simultaneously K_{linear} increased 4-fold.

An important parameter is the effective molarity (EM),[16,17] which is the concentration at which extension of linear dimer **lin-CxC•AyA** is as likely as cyclization to **cyc-CxC•AyA**; above this concentration linear self-assembly of trimers and higher oligomeric assemblies is favored. As indicated in Table 1 the EM value for **C8C**/**A22A** (0.060 mM) clearly stands out, showing a 16-fold improvement with respect to that of **C8C**/**A4A** (0.95 mM). These results indicate that the end-to-end distance of **AxA** plays a key role in determining the outcome of the complexation process. We expected this effect would enhance construction of supramolecular polymers ***lin*-[CxC•AyA]$_n$** using longer building blocks.

We also examined the self-assembly of the shorter bis(crown ether) host **C2C** with the C_{22} linked diammonium guest **A22A**. K_{linear} is higher for this system than for any of the other pairs (Table 1). The total number of methylene spacer units is 24 for **C2C**/**A22A**, and in terms of K_{cyclic} it falls between **C8C**/**A10A** (18 CH_2) and **C8C**/**A22A** (30 CH_2). The observed EM is essentially the same for **C2C**/**A22A** and **C8C**/**A22A**.

The NMR spectra of these dilute solutions were recorded over a temperature range from 285 to 313 K.[18] By use of van't Hoff plots ΔH values were evaluated over this temperature range. These results are summarized in Table 1. ΔH_{linear} values for complexes with **C8C** become more negative, while ΔH_{cyclic} values become less negative as the spacer length increases (Table 1, Figure 5b).

We interpret these results as being the result of an enthalpic penalty for cyclization in addition to the expected entropic penalty. Recent experimental[19] and theoretical[20] results for systems which contain semirigid linkages provide precedence for such observations. These workers found that for semirigid systems the enthalpic penalty for formation of a ring grew with the length of the species. In the present case rigidity is brought about by the dibenzylammonium moieties themselves and the fact that the charged sites Coulombically repel each other. ΔH_{cyclic} represents the difference in enthalpy between the linear and cyclic dimers. If it is assumed that the enthalpic stabilization from forming the cyclic species from the linear is equivalent to that in forming the linear species from its components, as the model systems indicate for forming [2]- and [3]pseudorotaxanes, then ΔH_{cyclic} represents the difference between that value and the enthalpic penalty. In other words the enthalpic penalty,

(15) Stockmayer (ref 16) has shown that under equilibrium conditions the concentration of unstrained rings decreases exponentially (5/2 power) with ring size. Hence the likelihood of the cyclic tetramer is $1/2^{5/2} = 1/6$ and the cyclic hexamer 1/16 that of the cyclic dimer. On this basis the contribution of larger cyclic species is considered minimal.

(16) Early on in the macromolecular field, because of the importance of cyclization as a competitive side reaction for step-growth polymerizations, Stockmayer (Jacobson, H.; Stockmayer, W. H. *J. Chem. Phys.* **1950**, *18*, 1600−1606) devised a treatment relating the concentration at which intra- and intermolecular reactions are equally probable, c_{eq}, to the mean squared end-to-end distance $\langle r^2 \rangle$: $c_{eq} \alpha \langle r^2 \rangle^{3/2}$. This relationship has been verified in a number of experimental studies, e.g., Heath, R. E.; Wood, B. R.; Semlyen, J. A. *Polymer* **2000**, 1487−1495 and references therein. This means that the tendency for cyclization decreases with increasing ring size.

(17) Kirby, A. J. *Adv. Phys. Org. Chem.* **1980**, *17*, 183−278. For examples of applications of this concept see: Illuminati, G.; Mandolini, L. *Acc. Chem. Res.* **1981**, *14*, 95−102. Mandolini, L. *Adv. Phys. Org. Chem.* **1986**, *22*, 1−111. Ercolani, G. *J. Phys. Chem. B* **1998**, *102*, 5699−5703.

(18) At lower temperatures linear oligomers (***lin*-[CxC•AyA]$_{n\geq 2}$**) were formed, complicating the analyses.

(19) Bonnet, G.; Krichevsky, O.; Libchaber, A. *Proc. Natl. Acad. Sci. U.S.A.* **1998**, *95*, 8602−8606. Goddard, N. L.; Bonnet, G.; Krichevsky, O.; Libchaber, A. *Phys. Rev. Lett.* **2000**, *85*, 2400−2403.

(20) Dua, A.; Cherayil, B. J. *J. Chem. Phys.* **2002**, *117*, 7765−7773.

Table 1. Association Constants (K_{linear}, K_{cyclic}:Scheme 4), and Enthalpies for Linear and Cyclic Dimerization of Ditopic Hosts **CxC** with Ditopic Guests **AyA** [$(CD_3)_2CO$:$CDCl_3$ (1/1, v/v)]

H/G *x*/*y*	$K_{linear,\ 295K}$[a] (M^{-1})	$\Delta G_{linear,\ 295K}$ (kcal/mol)	$K_{cyclic,\ 295K}$[a]	$\Delta G_{cyclic,\ 295K}$ (kcal/mol)	EM_{295K}[b] (mM)	ΔH_{linear}[c] (kcal/mol)	ΔH_{cyclic}[c] (kcal/mol)	$\Delta H_{cyclic\ penalty}$[d] (kcal/mol)
8/4	$1.3 \pm 0.3 \times 10^3$	-4.2 ± 0.1	2.5 ± 0.4	-0.54 ± 0.10	0.96 ± 0.50	-8.0 ± 0.6	-8.6 ± 1.0	-0.6 ± 1.6
8/10	$3.7 \pm 0.7 \times 10^3$	-4.9 ± 0.2	1.7 ± 0.3	-0.31 ± 0.10	0.23 ± 0.10	-11 ± 2	-3.7 ± 0.1	$+7 \pm 2$
8/22	$5.2 \pm 0.6 \times 10^3$	-5.0 ± 0.1	0.62 ± 0.03	$+0.28 \pm 0.03$	0.060 ± 0.010	-10 ± 3	-2.1 ± 0.6	$+8 \pm 3$
2/22	$8.9 \pm 0.9 \times 10^3$	-5.3 ± 0.1	0.86 ± 0.14	$+0.088 \pm 0.10$	0.050 ± 0.015	–	–	–

[a] $K_{linear} = [$***lin*-CxC•AyA**$]/[$**CxC**$][$**AyA**$]$. $K_{cyclic} = [$***cyc*-CxC•AyA**$]/[$***lin*-CxC•AyA**$]$. ±-Values represent standard deviations for determinations using three independently prepared solutions at concentrations of 0.20 and 0.40 mM. [b] Calculated from $EM = K_{cyclic}/2K_{linear}$. This assumes that the equilibrium constant for addition of a unit of either **CxC** or **AyA** to linear dimer ***lin*-CxC•AyA** is identical to the measured K_{linear}. EM is the concentration of building blocks **CxC** and **AyA** at which the total concentration of trimers ***lin*-CxC•AyA•CxC** and ***lin*-AyA•CxC•AyA** is equal to the concentration of cyclic dimer ***cyc*-CxC•AyA**. Since $K_{linear} = [$***lin*-CxC•AyA•CxC**$]/[$***lin*-CxC•AyA**$][$**CxC**$] = [$***lin*-AyA•CxC•AyA**$]/[$***lin*-CxC•AyA**$][$**AyA**$]$ and $K_{cyclic} = [$***cyc*-CxC•AyA**$]/[$***lin*-CxC•AyA**$]$, when $[$***lin*-CxC•AyA•CxC**$] + [$***lin*-AyA•CxC•AyA**$] = [$***cyc*-CxC•AyA**$]$, $[$**CxC**$] = [$**AyA**$] = EM = K_{cyclic}/2K_{linear}$. [c] ±-Values represent errors estimated for slopes of van't Hoff plots of association constants determined using the three independently prepared solutions over the temperature range 285−313 K, $r^2 \geq 0.97$. At lower temperatures higher linear species (***lin*-[CxC•AyA]$_n$**, $n \geq 2$) formed, preventing measurements of K_{linear} and K_{cyclic}. [d] $\Delta H_{cyclic\ penalty} = \Delta H_{cyclic} - \Delta H_{linear}$. ±-Values represent errors derived by summing the errors in the individual terms on the right.

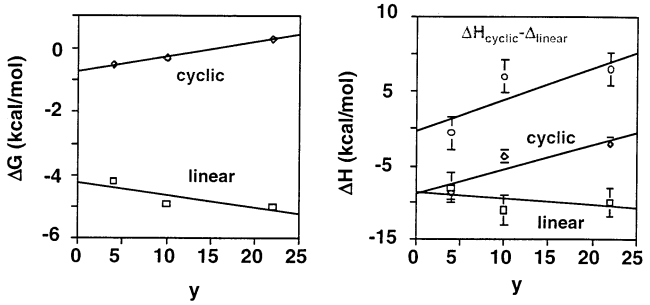

Figure 5. (Left) Dependence of ΔG_{linear} and ΔG_{cyclic} on *y* for complexation of **C8C** and **AyA**. (Right) Dependence of ΔH_{linear}, ΔH_{cyclic} and $\Delta H_{linear} - \Delta H_{cyclic}$ on *y* for complexation of **C8C** and **AyA**. Data from Table 1.

$\Delta H_{cyclic\ penalty}$, is $\Delta H_{cyclic} - \Delta H_{linear}$. This parameter indeed increases linearly as the length of **AyA** increases (Table 1, Figure 5b).

IV. Non-Covalent Polymers from CxC and AyA. IV. a. Theoretical Expectations. A relationship among the association constant between **CxC** and **AyA**, their concentrations and the average degree of polymerization, *n*, of the resultant ***lin*-[CxC•AyA]$_n$**, is easily derived as follows, under the assumptions that the same average association constant holds for each successive step (isodesmic)[21] and that cyclic species can either be ignored or taken into account. Consider the generalized equilibrium of Scheme 5, in which the concentrations of the two homoditopic species are equal:

We can write $K = [H/G]/[H][G] = [H/G]/[H]^2$.

If we now define $p =$ extent of complexation,

$K = p[H]_o/(1 - p)^2[H]_o^2$.

Solving this quadratic equation leads to

$1 - p = \{(1 + 2K[H]_o)^{1/2} - 1\}/2K[H]_o$

This relationship allows us to use the well-known Carothers equation,[22] which relates *n* to the extent of conversion of functional groups, in this case topological functional groups:

$$n = 1/(1 - p) = 2K[H]_o/\{(1 + 2K[H]_o)^{1/2} - 1\}$$

Now if $2K[H]_o \gg 1$, $n = 2K[H]_o/\{(2K[H]_o)^{1/2} - 1\}$

and if $(2K[H]_o)^{1/2} \gg 1$, $n = (2K[H]_o)^{1/2}$ (1)

In this system $[H]_o = 2[H{-}H]_o$.[23]

Therefore, since K_{linear} is on the order of $5.0 \times 10^3\ M^{-1}$ (Table 1), in the absence of cyclics, at 1.0 M concentration of **CxC** and **AyA** we would expect $n = [(2)(1.0\ M)(2)(5.0 \times 10^3\ M^{-1})]^{1/2} = 1.4 \times 10^2$.

IV. b. NMR Studies. By increasing the equimolar concentrations as eq 1 requires to produce high supramolecular mass assemblies, we then proceeded to construct linear arrays *lin*-[Ax•Cy]$_n$, using the sets of complementary homoditopic molecules, **CxC** and **AyA**, as represented in cartoon form in Scheme 4.

The ^{1}H NMR spectra of equimolar solutions of **C8C** and **A10A** in acetone-d_6/chloroform-*d* (1/1, v/v) contained three sets of signals for the NCH_2 protons (e.g., see Figure 6d). As noted above, two of these are attributed to complexed moieties, while the other set corresponds to the signals for uncomplexed species. The two sets of signals for complexed NCH_2 units arise from two different pseudorotaxane structures, the cyclic dimer ***cyc*-C8C•A10A**, and linear dimer ***lin*-C8C•A10A** and linear species ***lin*-[C8C•A10A]$_n$** (Scheme 4), the latter two being indistinguishable.[25] Cyclic dimer ***cyc*-C8C•A10A** was preferentially formed in equimolar dilute solutions (<1.0 mM, see Figure 6c).

The ^{1}H NMR spectra (Figure 6) recorded at different equimolar concentrations of **C8C** and **A10A** in acetone-d_6:chloroform-*d* (1:1, v:v) revealed that both the ratio of ***cyc*-C8C•A10A** to ***lin*-[C8C•A10A]$_n$** and the extent of aggregation,

Scheme 5. Generalized Representation of Self-Assembly of Linear Supramolecular Polymer from Complementary Homoditopic Building Blocks. H = host; G = guest; H/G = complex

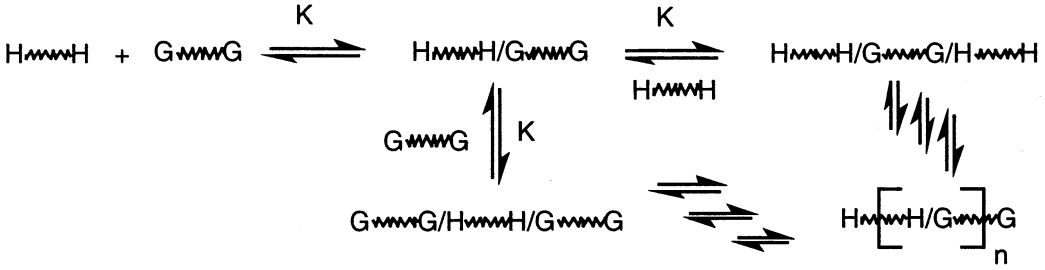

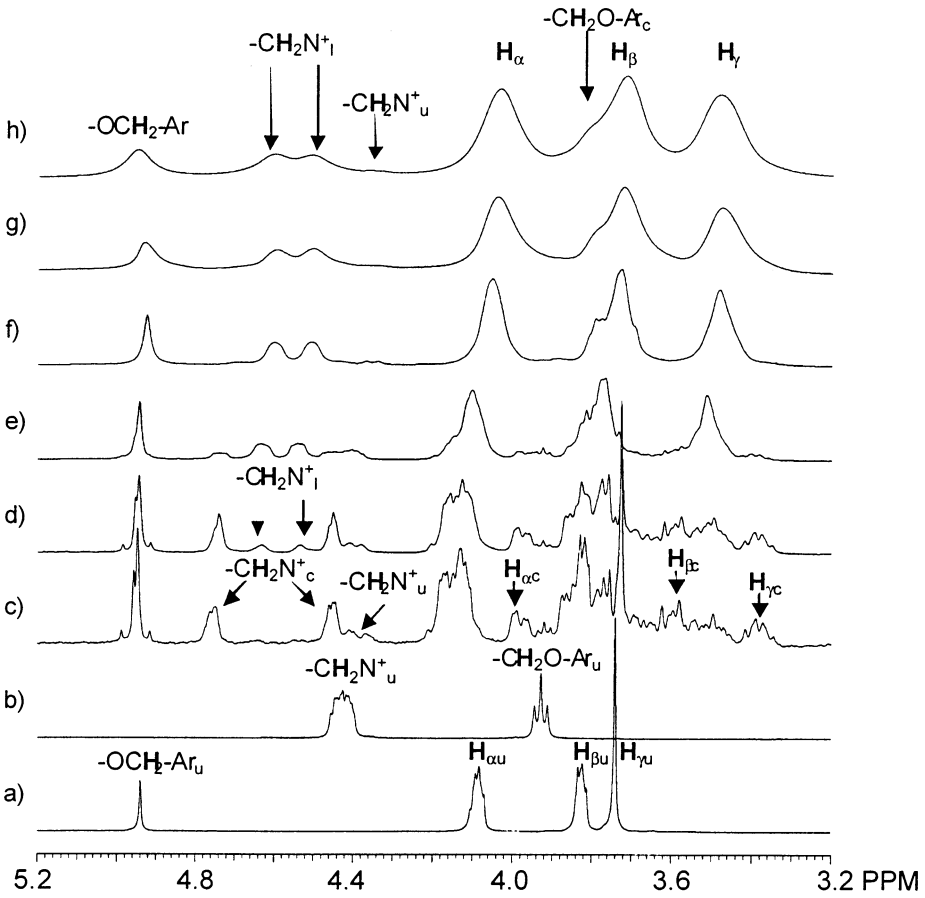

Figure 6. Partial ^{1}H NMR spectra of solutions of **C8C** and **A10A** at (a) 10/0, (b) 0/10 mM/mM, and equimolar solutions at (c) 1.0×10^{-3}, (d) 1.0×10^{-2}, (e) 1.0×10^{-1}, (f) 0.50, (g) 1.0, and (h) 2.0 M (400 MHz, acetone-d_6:chloroform-*d* (1:1, v:v), 22 °C). The three sets of NCH_2 signals are for (1) uncomplexed moieties, i.e., end groups, (denoted by "u") in **A10A**, ***lin*-[A10A•C8C]$_n$•A10A** and ***lin*-[C8C•A10A]$_n$**, (2) complexed moieties (denoted by "l") in ***lin*-[C8C•A10A]$_n$**, ***lin*-[A10A•C8C]$_n$•A10A** and ***lin*-[C8C•A10A]$_n$•C8C**, and (3) complexed moieties in ***cyc*-C8C•A10A** (denoted by "c"). These assignments were confirmed by the results presented in Figure 3.

n, of the latter are concentration-dependent as expected. At the highest equimolar concentration we examined (2.0 M), the signals for the cyclic dimer **cyc-C8C•A10A** are no longer observed (Figure 6h), indicating its absence. It is noteworthy that linear covalent polymerization is highly favored over cyclization at high concentrations, e.g., 1.0 M.[16,26] Therefore, the assumption of the absence of the oligomeric cyclic complexes is believed to be valid in the more concentrated solutions.[15] Since the concentrations of the end-groups in the supramolecular polymer ***lin*-[C8C•A10A]$_n$** can be determined by integrating the signal for uncomplexed NCH_2 moieties, one can estimate its average molecular weight (Table 2). For instance, in the 2.0 M equimolar solution $M_n = 18$ kDa ($n = 9.1$). Substantially broadened signals in Figure 6, g and h, support the formation of large supramolecular polymers ***lin*-[C8C•A10A]$_n$** in solution.

Equimolar solutions of **C8C** and the complementary homoditopic molecules **A4A** and **A22A** were also characterized by ^{1}H NMR spectroscopy in acetone-d_6:chloroform-*d* (1:1, v:v). In the case of **C8C** and **A4A**, the spectra[10] confirmed that the efficiency of formation of the cyclic dimer ***cyc*-C8C•A4A** was greater than that of ***cyc*-C8C•A10A** from **C8C** and **A10A** (Table 2) at all concentrations. Equimolar solutions higher than 1.0 M could not be achieved due to the poor solubility of the shorter **A4A**. In the equimolar 0.5 M solution of **C8C** and **A4A** the supramolecular polymer ***lin*-[C8C•A4A]$_n$** has an average molecular weight (M_n) of 6.1 kDa, which is nearly a 2-fold decrease with respect to that of ***lin*-[C8C•A10A]$_n$** (Table 2). These observations are consistent with the dilute solution studies above (Table 1) in which it was demonstrated that the shorter the end-to-end distance of the components, the higher the percentage of the cyclic dimer complex (***cyc*-CxC•AyA**) formation

In contrast, the spectra of equimolar solutions of **C8C** and **A22A** (Figure 7) indicated quite convincingly that the formation of the cyclic dimer complex ***cyc*-C8C•A22A** was reduced compared to the systems **C8C•A4A** and **C8C•A10A** (Table 2).

(21) This term refers to linear self-assembly processes in which the successive equilibrium constants are all the same. Other models include systematic diminution of successive association constants, the attenuated K model; see Martin, R. B. *Chem. Rev.* **1996**, *96*, 3043−3064.
(22) Carothers, C. H. *Trans. Faraday Soc.* **1936**, *32*, 39−53.
(23) Other authors have derived similar equations: Meijer et al., ref 24; Lehn, ref 4, though not explicitly given.
(24) Sijbesma, R. P.; Beijer, F. H.; Brunsveld, L.; Folmer, B. J. B.; Hirschberg, J. H. K. K.; Lange, R. F. M.; Lowe, J. K. L.; Meijer, E. W. *Science* **1997**, *278*, 1601−1604.
(25) Note that linear dimer ***lin*-CxC•AyA** in fact is identical to ***lin*-[AyA•CxC)]$_n$** $n = 1$. ***lin*-CxC•AyA** is shown explicitly for clarity. Under isodesmic conditions the concentrations of ***lin*-[CxC•AyA]$_n$CxC** and ***lin*-[AyA•CxC)]$_n$•AyA** will always be equal when the concentrations of **CxC** and **AyA** are equal. Note that species ***lin*-[CxC•AyA]$_n$•CxC** and **lin-(AyA•CxC)$_n$•AyA** cannot directly cyclize, unlike the case of oligomers derived from complementary heteroditopic monomers; this lack of direct cyclizability of 50% of the species present is a previously unrecognized advantage of the homoditopic pair approach.
(26) Flory, P. J. *Principles of Polymer Chemistry*; Cornell University Press: Ithica, NY, 1953; pp 317−346.

Table 2. Analyses of Percentages of Ammonium Ion Moieties in Cyclic Dimers = CD (*cyc*-**CxC•AyA**) and Supramolecular Polymers = SP (*lin*-[**CxC•AyA**]$_n$) and the Average Number of Repeat Units, *n*, in SP Derived from Ditopic Hosts **CxC** and Ditopic Guests **AyA**

H/G *x*/*y*	equimolar concentration (M)	% in CD at +22/–40°C[a]	% uncomp. at +22/–40°C[a]	*n*[b] of SP at +22/–40 °C	M_n of SP[c] at +22/–40 °C (kDa)	predicted *n* of SP[d] @ 22 °C
8/4	0.50	17	13	3.2 ± 0.6	6.1 ± 1.2[f]	51 ± 7
	0.10	25	14	2.7 ± 0.4	5.1 ± 0.8[f]	23 ± 3
	1.0×10^{-2}	78	7	1.6 ± 0.6	3.0 ± 1.2[f]	7.2 ± 0.9
	1.0×10^{-3}	86	9	0.78 ± 0.28	1.5 ± 0.6[f]	–
8/10	2.0	0/–[e]	5.5/–[e]	9.1 ± 3.8/–[e]	18 ± 8/–[e,g]	$1.7 \pm 0.2 \times 10^2$
	1.0	3.4/–[e]	6.4/–[e]	7.5 ± 2.7/– [e]	15 ± 5/–[e,g]	$1.2 \pm 0.1 \times 10^2$
	0.50	12/15	7.9/5.1	5.6 ± 1.6/8.3 ± 4.1	11 ± 3/16 ± 8[g]	86 ± 9
	0.10	23/27	20/5.4	1.9 ± 0.2/6.8 ± 3.1	3.8 ± 0.3/13 ± 6[g]	38 ± 4
	1.0×10^{-2}	66/81	16/4.3	1.1 ± 0.2/2.2 ± 1.6	2.2 ± 0.4/4.4 ± 3.2[g]	12 ± 1
	1.0×10^{-3}	72/94	20/2.3	0.70 ± 0.12/1.3 ± 6.2	1.4 ± 0.2/2.6 ± 12.4[g]	3.8 ± 0.4
8/22	1.0	0	4.4	11 ± 6.6	24 ± 14[h]	$1.4 \pm 0.1 \times 10^2$
	0.50	0	4.7	11 ± 5.8	24 ± 12[h]	$1.0 \pm 0.1 \times 10^2$
	0.10	8.3	20	2.3 ± 0.3	4.9 ± 0.6[h]	46 ± 3
	1.0×10^{-2}	28	34	1.1 ± 0.1	2.4 ± 0.2[h]	14 ± 1
	1.0×10^{-3}	38	43	0.72 ± 0.06	1.5 ± 0.2[h]	4.6 ± 0.3
2/22	0.50	0/–[e]	1.8/–[e]	28 ± ~10/–[e]	58 ± 20/–[e,i]	$1.3 \pm 0.3 \times 10^2$
	0.10	17/10	9.2/4.3	4.5 ± 0.7/10 ± 6.5	9.3 ± 2.4/21 ± 14[i]	60 ± 3
	1.0×10^{-2}	38/55	24/4.7	1.3 ± 0.2/4.8 ± 2.8	2.7 ± 0.3/9.9 ± 5.7[i]	19 ± 1
	1.0×10^{-3}	44/63	39/13	0.72 ± 0.06/1.4 ± −0.3	1.5 ± 0.1/2.9 ± 0.6[i]	6.0 ± 0.3
8/EO35[j]	0.10	0	45	1.1 ± 0.1	3.7 ± 0.2[k]	–
	1.0×10^{-2}	0	77	0.65 ± 0.02	2.2 ± 0.1[k]	–
	1.0×10^{-3}	0	100	0	–	–

[a] Calculated from the ^{1}H NMR spectra of equimolar solutions (acetone-d_6/chloroform-*d*, 1/1, v/v) of **CxC** and **AyA**. Typically [*cyc*-**CxC•AyA**] was determined by direct integration of the NCH_2 signals of the cyclic species vs the total of all of the NCH_2 signals (checked vs the $ArOCH_2$ signals) and/or the H_y signals for the cyclic species vs the total of all of the NCH_2 signals. Typically the uncomplexed NCH_2 signals were determined either by direct integration of the uncomplexed ends of ***lin*-CxC•AyA** and ***lin*-[CxC•AyA]$_n$** and uncomplexed **AyA** vs the total of all of the NCH_2 signals or by difference between the complexed NCH_2 signals and twice the integral for the $ArOCH_2$ signals. Errors are estimated to be ±2%. [b] *n* was determined by solving the expression: $n = [100 - (\%$ of ammonium ion units in ***lin*-CxC•AyA**$)]/2(\%$ uncomplexed ammonium ion units). Errors cited are the average deviations using 2% errors in % ***lin*-CxC•AyA** and % uncomplexed. The maximum values were determined using the observed % ***lin*-CxC•AyA** less 2% and the observed % uncomplexed less 2%. The minimum values were determined using the observed % ***lin*-CxC•AyA** plus 2% and the observed % uncomplexed plus 2%. There is larger error toward the maximum values. [c] Errors cited are the average deviations of the maximum and minimum values calculated using the maximum and minimum values of *n* based on 2% errors as noted in footnote b. There is larger error toward the maximum values. [d] Based on eq 1 and K_{linear} value of Table 1; recall that eq 1 assumes no cyclics form. Therefore, this value is a reference point for the situation in which no cyclic forms and K_{linear} is invariant with concentration. No calculations were done when the inequalities assumed in eq 1 were violated. [e] The spectra recorded at lower temperatures exhibited severe signal broadening, preventing accurate signal integration. [f] The number average molecular weight (M_n) of the aggregate ***lin*-[C8C•A4A]$_n$** was calculated using $M_n = n$(1896 Da). [g] The number average molecular weight (M_n) of the aggregate ***lin*-[C8C•A10A]$_n$** was calculated using $M_n = n$(1980 Da). [h] The number average molecular weight (M_n) of the aggregate ***lin*-[C8C•A22A]$_n$** was calculated using $M_n = n$(2148 Da). [i] The number average molecular weight (M_n) of the aggregate ***lin*-[C2C•A22A]$_n$** was calculated using $M_n = n$(2064 Da). [j] In $CDCl_3$. [k] The number average molecular weight (M_n) of the aggregate ***lin*-[C8C•AEO35A]$_n$** was calculated using $M_n = n$(3346 Da).

More importantly, in equimolar solutions of **C8C** and **A22A** at greater than 0.5 M the cyclic dimer ***cyc*-C8C•A22A** was not detected (Table 2, Figure 7e). From end group analysis, the average molecular weight of supramolecular polymer ***lin*-[C8C•A22A]$_n$** is 24 kDa at 0.5 M; 2.0 M solutions could not be made due to the limited solubility of **A22A**.

Finally solutions of the shortest bis(crown ether) **C2C** and the longest diammonium salt **A22A**, as expected on the basis of the EM results of Table 1, yielded the largest linear aggregates. The highest degree of "noncovalent polymerization", *n*, was observed at 0.5 M concentrations, forming ***lin*-[C2C•A22A]$_n$** with a supramolecular molar mass of 58 kDa at ambient temperature. Again, the limited solubility of **A22A** did not allow higher concentrations to be studied.[27]

As expected on the basis of the low K_a observed in the model system **1a**/**AEO35A** noted above, homoditopic host **C8C** and homoditopic guest **AEO35A** showed very small extents of complexation as measured by the NCH_2 signals of **AEO35A**. At 22 °C in equimolar 100 mM $CDCl_3$ solutions only 55% complexation was observed versus 86, 80, and 80%, respectively, for **C8C** with **A4A**, **A10A**, and **A22A** each at 100 mM in the less polar solvent $CDCl_3$:CD_3COCD_3 (1:1, v:v). Furthermore, at 1.0 mM in $CDCl_3$ *no* complexation was observed for **C8C** and **AEO35A** (Table 2).

The error bars for *n* and M_n in Table 2 are large. This is an intrinsic problem in using NMR spectroscopy for end group analysis of polymeric systems. Note that as *n* increases, the error increases exponentially. Assuming that the error in end group determination is 2% absolute, at $n = 25$ the range would be from 17 to 50. In many cases the error will be larger than this. Therefore, NMR spectroscopy is at best a qualitative tool for study of such supramolecular polymers. Other physical methods are needed to establish the polymeric nature of the assemblies.

Nonetheless it is clear from Table 2 that degrees of noncovalent polymerization, *n*, are much less than predicted by eq 1 above, notwithstanding the intrinsic errors. For example, with **C8C**/**A22A** at 1.0 M the experimental *n* value is only 20% of that calculated by eq 1. Such comparisons for other results in Table 2 indicate a diminution in the effective association constant with increasing concentrations. In model monotopic systems we have also noted such concentration dependences.[28] A possible contributing factor is "exo complexation", i.e., non-pseudorotaxane hydrogen bonding of the crown ether and ammonium salt moieties;[13] this consumes "free" species and reduces their true concentrations, increasingly as total concentra-

(27) Pseudorotaxane formation involving **A22A** was found to be time dependent with both **C8C** and **C2C**. Approximately 18−24 h were required for equilibration.

(28) Jones, J. W.; Huang, F.; Gibson, H. W. *J. Am. Chem. Soc.*, submitted.

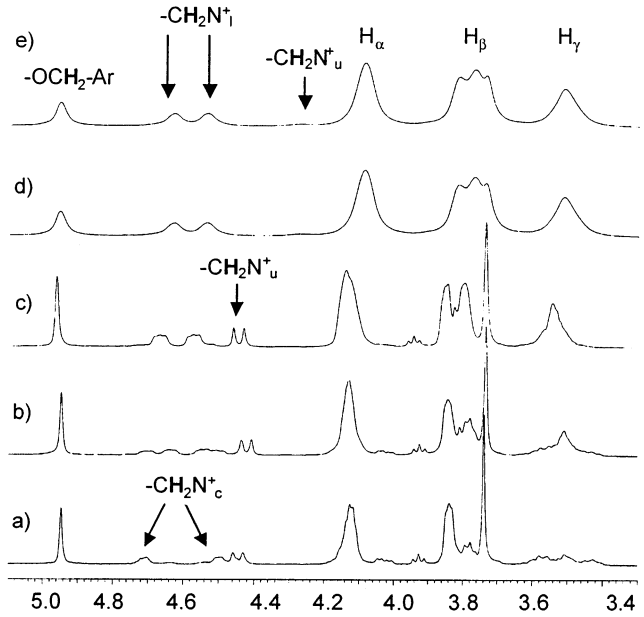

Figure 7. The ^{1}H NMR spectra of equimolar solutions of **C8C** and **A22A** at (a) 1.0×10^{-3}, (b) 1.0×10^{-2}, (c) 0.10, (d) 0.50, and (e) 1.0 M each (400 MHz, acetone-d_6:chloroform-*d* (1:1, v:v), 22 °C). The three sets of NCH_2 signals are for 1) uncomplexed moieties, i.e., end groups, (denoted by "u") in **A22A**, ***lin*-[A22A•C8C]$_n$•A22A** and ***lin*-[C8C•A22A]$_n$**, (2) complexed moieties (denoted by "l") in ***lin*-[C8C•A22A]$_n$**, ***lin*-[A22A-•C8C]$_n$•A22A** and ***lin*-[C8C•A22A]$_n$•C8C**, and (3) complexed moieties in ***cyc*-C8C•A22A** (denoted by "c").

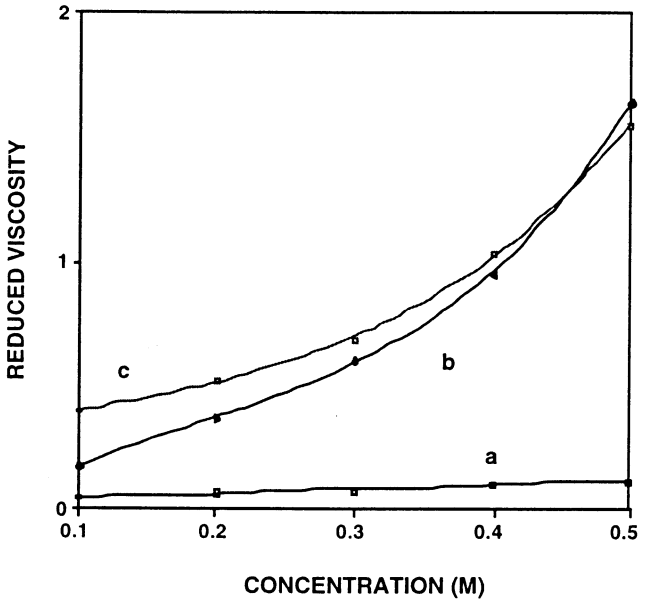

Figure 8. Reduced viscosity as a function of equimolar host and guest concentrations in acetone:chloroform (1:1, v:v) at 22 °C for (a) **MC8MC** and **A10A**, (b) **C8C** and **A10A**, and (c) **C2C** and **A22A**. Error bars are estimated to be 0.2% at 0.1 M, but perhaps as high as 5% at 0.5 M because of capillary absorption effects.

tions increase. On the basis of the Debeye−Hückel treatment activity coefficients are sharply dependent on ionic concentration in solvents of low dielectric constant.[29] Clearly at concentrations as high as 1 or 2 M the ionic strength effect may substantially affect the activity coefficients and the apparent association constants. As a result of these effects an "attenuated K" model is probably more appropriate than the isodesmic treatment of eq 1.[21] These effects taken together present a serious challenge in analyses of equilibria involving charged species for construction of supramolecular polymers in organic media.

IV. c. Solution Viscosity. For direct physical evidence of the formation of large self-assembled noncovalent polymers, we turned to viscometry. A plot of reduced viscosity versus concentration of equimolar solutions of **C8C** and **A10A** in acetone-d_6:chloroform-*d* (1:1, v:v) is nonlinear (Figure 8b), reflecting the increasing size of the supramolecular polymer ***lin*-[C8C•A10A]$_n$** with concentration as shown by the ^{1}H NMR data. In fact, the viscosities of 1.0 and 2.0 M equimolar solutions were too high to measure by this method.

On the other hand, a completely different solution viscosity profile was observed for equimolar solutions of **MC8MC**, a constitutional isomer of **C8C**, and **A10A** (Figure 8a). It should be noted that the ^{1}H NMR spectrum of an equimolar solution of **C2C** and dibenzylammonium hexafluorophosphate (**6**) at 10 mM in the same solvent system displayed no sign of complexation, i.e., did not show extra sets of signals due to slow exchange or changes in the chemical shifts due to fast exchange. The *m*-phenylene linkage in the crown ether moieties of **MC8MC** prevents or at least very strongly retards pseudorotaxane formation.[30] In the viscosity plot a straight line with low slope (Figure 8a) is consistent with the ^{1}H NMR observation that there is little or no complexation between **MC8MC** and **A10A** in solution. It also indicates that the ionic strength per se has a negligible effect on viscosity under these experimental conditions. Therefore, the sharp increases in viscosity at higher concentrations of **C8C**/**A10A** and **C2C**/**A22A** (Figure 8c) are reflective of aggregation, producing structures of large hydrodynamic volume, i.e., ***lin*-[C8C•A10A]$_n$** and ***lin*-[C2C•A22A]$_n$**.

Cates and Candau have derived theoretical relationships for the reduced viscosity of self-assembled noncovalent polymers comprised of surfactant molecules in aqueous media as a function of concentration.[31] According to this mean field theory if the association constants are high and the lifetimes of the assemblies exceed the reptation times, a plot of log(reduced viscosity) vs log(total concentration) should have a slope of 3.5−3.7. Such log−log plots for **MC8MC**/**A10A**, **C8C**/**A10A**, and **C2C**/**A22A** have slopes of 1.48, 2.83, and 2.64, respectively. The fact that the slopes of the latter two systems are less than the theoretical values may reflect several factors. First of all, Cates and Candau note that for their systems in water there was a strong inverse dependence of the exponent (slope) on salt concentration.[31] In our systems in organic solvents this effect would be expected to be exaggerated, since one of the components is in fact ionic and the concentrations are high. In one reported experiment in an organic solvent an exponent

(29) Glasstone, S.; Lewis, D. *Elements of Physical Chemistry*; D. van Nostrand Co., Inc.: New York, 1960; pp 507−516.

(30) Other workers have demonstrated that **MC8MC** does form a complex with dibenzylammonium hexafluorophosphate, but with an immeasurably (by NMR) low K_a: Ashton, P. R.; Bartsch, R. A.; Cantrill, S. J.; Hanes, R. E., Jr.; Hickingbottom, S. K.; Lowe, J. N.; Preece, J. A.; Stoddart, J. F.; Talanov, V. S.; Wang, Z.-H. *Tetrahedron Lett.* **1999**, *40*, 3661−3664. Cantrill, S. J.; Fulton, D. A.; Heiss, A. M.; Pease, A. R.; Stoddart, J. F.; White, A. J. P.; Williams, D. J. *Chem. Eur. J.* **2000**, *6*, 2274−2287.

(31) Cates, M. E. *Macromolecules* **1987**, *20*, 2296−2300. Cates, M. E.; Candau, S. J. *J. Phys. Condens. Matter* **1990**, *2*, 6869−6892. It should be noted that although this theoretical approach is still in use (Narayanan, J.; Urbach, W.; Langevin, D.; Manohar, C.; Zana, R. *Phys. Rev. Lett.* **1998**, *81*, 228−231), it is not without its peculiarities and controversy (Aliotta, F.; Sacchi, M. *Colloid Polym. Sci.* **1997**, *275*, 910−921. Köper, G. J.; van der Ploeg, J. P. O. M.; Cirkel, P. A. *Prog.Colloid Polym. Sci.* **1997**, *1055*, 294−297).

Table 3. Supramolecular Formulas, Calculated Supramolecular Weights, and Observed (MS) Mass/Charge Ratios of Complexes from Homoditopic Species **C8C** and **A10A**

structure	calcd MW	obs *m/z*[a]	obs *m/z*[b]
[A10A-PF_6]$^+$	711.4	711.3[a1]	
[**C8C•A10A**-$2HPF_6$]$^{2+}$	1686.9		844[b1]
[**C8C•A10A**-PF_6-HPF_6-DB24CH_2OOCCH_2]$^+$	1168.8		1169[b2]
[**C8C•A10A**-PF_6-HPF_6-DB24CH_2]$^+$	1226.7		1227[b3]
[**C8C•A10A**-$2PF_6$-DB24CH_2]$^+$	1227.7	1228[a2]	
[**C8C•A10A**-$2HPF_6$-$C_6H_5CH_2$]$^+$	1595.8		1596[b4]
[**C8C•A10A**-$2PF_6$-$C_6H_5CH_2$]$^+$	1597.8	1598.1[a3]	
[**C8C•A10A**-PF_6-HPF_6]$^+$	1687.9	1688.2[a4]	1688[b5]
[**C8C•A10A**-PF_6]$^+$	1833.9	1833.6[a5]	1834[b6]
[**A10A•C8C•A10A**-$4HPF_6$-$C_6H_4CH_2NH_2CH_2C_6H_5$]$^+$	2054.2		2054[b7]
[**A10A•C8C•A10A**-$2HPF_6$-PF_6-$C_6H_5CH_2$]$^+$	2307.3		2307[b8]
[**A10A•C8C•A10A**-PF_6-$2HPF_6$]$^+$	2398.3	2398.5[a6]	
[**C8C•A10A•C8C**-H-HPF_6]$^+$	2954.4	2954.0[a7]	
[**[C8C•A10A]$_2$•C8C**-$C_6H_5CH_2NH_2CH_2$]$^+$	4958.2	4959.0[a8]	

[a] MALDI-TOF mass spectrum recorded in the positive ion mode using 2,5-dihydroxybenzoic acid (2,5-DHB) matrix (Washington U); sample prepared in chloroform-acetone (1:1 v:v) at 2.0 M. 1) 9.6%, 2) 43%, 3) 7.8%, 4) 100%, 5) 5.8%, 6) 3.8%, 7) 2.5%, 8) 1.4%. "DB24" represents dibenzo-24-crown-8 moieties of **A10A**. [b] FAB mass spectrum recorded in the positive ion mode using 3-nitrobenzyl alcohol (3-NBA) as the matrix (Va Tech); sample prepared in chloroform-acetone (1:1 v:v) at 2.0 M. Same sample as in (a). 1) 85%, 2) 7%, 3) 10%, 4) 6.7%, 5) 100%, 6) 12%, 7) 1%, 8) 45%. "DB24" represents dibenzo-24-crown-8 moieties of **A10A**.

Table 4. Thermogravimetric Analyses of Pseudorotaxanes and Their Components[a]

sample	$T_{5\%}$[b] (°C)	other *T* (°C)/%	fragments lost (% th)
$(C_6H_5CH_2)_2NH_2^+PF_6^-$	220	*c*	
DB24C8	334	*d*	
1a•6[e]	210	270[f]/32	$C_6H_5CH_2NH_2$ (14) + HPF_6 (18)
A10A	224	343[f]/56	$O(CH_2)_{10}$ (20) + $2HPF_6$ (34)
C8C	340	461[f]/80	2 DB24C8−CH_2 (82)
C8C/**A10A**[g]	187	300[f]/15	$2HPF_6$ (15)
		462[f]/80	−

[a] Heating rate: 10 °C/min in N_2 unless otherwise noted. [b] Temperature of 5% weight loss. [c] Smooth weight loss to 3% residue at 289 °C. 32% weight loss corresponds to 271°C. [d] 40 °C/min; smooth weight loss to 3% residue at 409 °C. 32% weight loss corresponds to 392 °C. [e] Sample consisted of crystals of the pseudorotaxane complex grown by vapor diffusion of hexane into a chloroform solution 10 mM in both components. [f] Plateau value. [g] Sample prepared by evaporation of a chloroform−acetone (1:1 v:v) solution 1.0 M in both species.

(slope) of 1.9 was observed, a value lower than those obtained here.[32] Meijer et al. reported a slope of 3.76 for a nonionic H-bonded supramolecular polymer in chloroform. [23] Another possibility is that the lifetimes of the noncovalent polymers described here are shorter than their reptation times.

IV. d. Mass Spectrometry. Due to the highly ionic nature of the linear arrays and the normally used very polar matrixes, which tend to dissociate the complexes, mass spectrometry on samples prepared from ditopic host **C8C** and ditopic guest **A10A** did not reveal assemblies of high mass. As shown in Table 3 MALDI-TOF and FAB techniques detected only species ***lin*-[A10A•C8C]$_n$•A10A** containing up to five total building blocks, i.e., $n = 2$.

IV. e. Thermogravimetric Analysis (TGA). As shown in Table 4 TGA of samples prepared by evaporation of equimolar solutions of homoditopic host **C8C** and homoditopic guest **A10A** reflect the thermal stabilities of the two components. Results for the model system consisting of DB24C8 (**1a**) and dibenzylammonium hexafluorophosphate (**6**) are similar. Thermal decomposition of the secondary ammonium salt moieties of **A10A** gives HPF_6, and the resultant secondary amine is believed to attack the ester linkage of **C8C** to afford a polyamide and alcohol **2a**, as supported by ^{1}H NMR spectral results. The loss of HPF_6 occurs at lower temperatures in the pseudorotaxane complexes than in the ammonium salts by themselves; this is probably because the anions are separated spatially from the cations in the pseudorotaxanes and therefore not as tightly bound.

IV. f. Differential Scanning Calorimetry (DSC). Solid samples were prepared by freeze-drying 1.0×10^{-3}, 0.10, and 0.50 M equimolar solutions of **C8C** and **A10A** in acetone:chloroform (1:1, v:v) at −93 °C under high vacuum. The ^{1}H NMR spectra of equimolar solutions of **C8C** and **A10A** at 1.0×10^{-3}, 0.10, and 0.50 M in acetone-d_6:chloroform-*d* (1:1, v:v) were essentially unchanged from −40 to −60 °C (below this temperature the ^{1}H NMR spectra of the solutions could not be recorded due to partial freezing of the solvent). Thus, M_n's of the supramolecular polymer ***lin*-[A10A•C8C]$_n$** and the abundance of the cyclic dimer **cyc-C8C•A10A** in the freeze-dried samples were estimated by simple integration of relevant signals of the spectra recorded at −40 °C (Table 2). The samples were analyzed by DSC. To eliminate sample history, the freeze-dried samples were heated to 100 °C and cooled to 30 °C at 10 °C min^{-1}. They were heated at 10 °C min^{-1} and the DSC thermograms were recorded. The pure homoditopic molecules **C8C** and **A10A** were crystalline and thus revealed sharp first-order phase transitions. As a result of self-assembly, amorphous polymer ***lin*-[A10A•C8C]$_n$** with glass transition temperatures (T_g) of 57 and 59 °C, respectively, were formed from the 0.10 and 0.50 M samples with $M_n = 13$ and 16 kDa, respectively (Table 2). In the case of the 10 mM sample (81% cyclic dimer **cyc-C8CA10A**, Table 2), a high degree of crystallinity was observed by optical microscopy

IV. g. Film and Fiber Formation. Flexible, creasible, amorphous, and transparent films were cast from 1:1 stoichiometric solutions of **C8C** and **A10A** at concentrations >0.50 M. Such film properties can only result from entanglement of linearly connected macro-sized aggregates. Similarly, since a polymeric structure of high molecular weight is necessary for fiber formation, the scanning electron microscopic images (Figure 9) of a fiber drawn from a concentrated equimolar solution of **C8C** and **A10A** confirm the high degree of the linear chain extension in ***lin*-[C8C•A10A]$_n$**. Fibers of ***lin*-[C8C•A22A]$_n$**

(32) Schurtenberger, P.; Scartazzini, R.; Magid, L. J.; Leser, M. E.; Luisi, P. L. *J. Phys. Chem.* **1990**, *94*, 3695−3701.

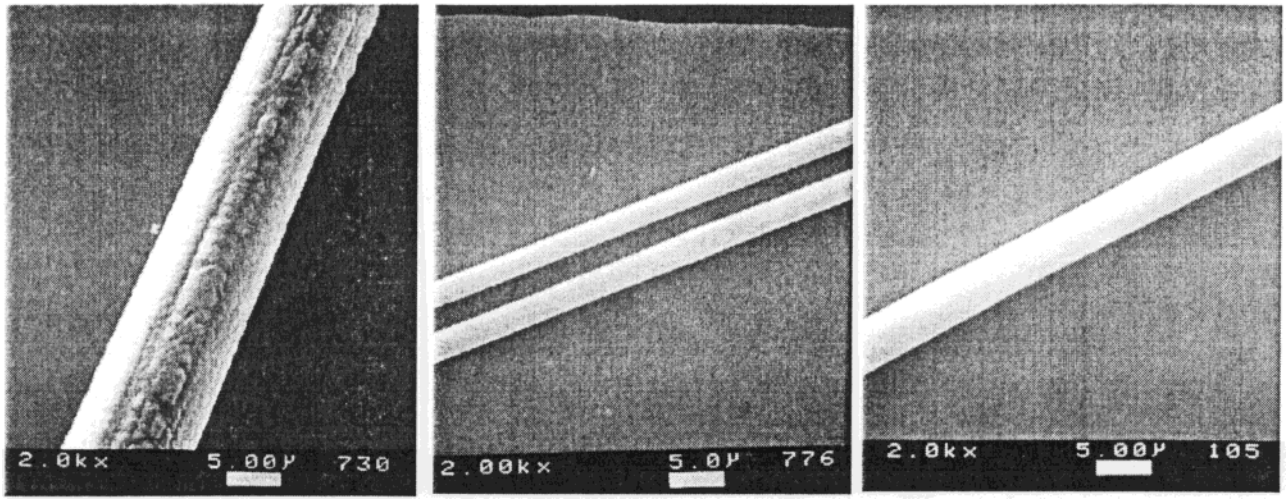

Figure 9. Scanning electron micrographs of (gold-coated) fibers pulled from concentrated solutions of (a) (left) **C8C** and **A10A**, (b) (center) **C8C** and **A22A**, and (c) (right) **C2C** and **A22A**. The scale bar in each micrograph is 5 μm.

and ***lin*-[C2C•A22A]$_n$** were also drawn from concentrated solutions of **C8C**/**A22A** and **C2C**/**A22A**, respectively. As shown in Figure 9, the morphology of these fibers was similar to that of those from ***lin*-[C8C•A10A]$_n$**. These fibers were formed in a manner analogous to dry spinning[33] used for covalently bonded macromolecules. Unfortunately, insufficient quantities prevented mechanical characterization of the films and fibers at this time.

Conclusions

In summary, linear (***lin*-CxC•AyA**) and cyclic (***cyc*-CxC•AyA**) dimeric complexes are preferentially formed in dilute equimolar solutions ($\leq$1 mM) of bis(crown ether)s **CxC** and diammonium salts **A4A** through **A22A**. Linear chain extension to ***lin*-[CxC•AyA]$_n$** is observed almost exclusively in concentrated equimolar solutions ($\geq$0.5 M) of homoditopic hosts **C8C** or **C2C** with homoditopic guests **A4A** through **A22A**. The solution behaviors of the self-organized supramolecular assemblies ***lin*-[CxC•AyA]$_n$** were characteristic of large linear aggregates as demonstrated by the viscosity experiments. Moreover, the preparation of films and fibers corroborates the polymeric nature of the self-organized supramolecules. Freeze-drying equimolar solutions yielded linear assemblies ***lin*-[CxC•AyA]$_n$** as amorphous solids. The efficiencies of the formation of the noncovalent polymers from complementary homoditopic molecules increased with increasing end-to-end distance of the building blocks. These studies provide proof of principle that self-assembly via pseudorotaxane formation can produce noncovalent polymers; however, there is a caveat in that exo complexation[13] and ionic strength[28] effects greatly reduce the effectiveness of pseudorotaxane formation at high concentrations. Future improvements will involve host−guest pairs with higher association constants to provide higher supramolecular weights.

Experimental Section

The 400 MHz ^{1}H NMR spectra were recorded with tetramethylsilane (TMS) as an internal standard. Deconvolution of the partially overlapping signals for "lu" and "cc" of dilute solutions of **CxC**/**AyA** of Figure 4, a and b, were carried out using Lorentzian line shapes in the Varian NMR Software package, version 6.1B.; the peak maxima were assigned using the positions of the shoulders due to "lu". The integration values from the deconvolutions were checked by taking the total integral in the region 4.35 to 4.45 ppm and subtracting from it the integral for the other "cc" signal at 4.75 ppm. Reduced viscosities were measured on a Cannon-Ubbelohde semi-micro dilution viscometer with 200 centipoise inner diameter capillary. Differential scanning calorimetry (DSC) was performed under a nitrogen purge using indium as the calibration standard. For scanning electron microscopy (SEM) fibers were drawn from concentrated solutions using a boiling stick or tweezers and placed on the mounting grid; the copper substrate was sputtered with gold after sample deposition and before exposure to the electron beam. Mass spectra were provided by the Washington University Mass Spectrometry Resource, an NIH Research Resource (Grant No. P41RR0954). Dialdehydes **3a** and **3b** were prepared by the procedures reported in the literature.[34] We previously reported[7a] syntheses of **1a**, **1b**, **2a**, **2b**, **C8C**, **MC8MC**, **4b**, **5b**, **A10A**, and **7a**.

Acknowledgment. We are grateful to the National Science Foundation for support of this work through Grant CHE-9521738. We thank Thomas Glass for expert assistance in obtaining the NMR spectra and Professor James McGrath for use of his thermal analysis equipment.

Supporting Information Available: Procedures for synthesis of **C2C**, **3c**, **3d**, **4a**, **4c**, **5a**, **5c**, **5d**, **A4A**, **A22A**, and **AEO35A**; ^{1}H NMR and mass spectra (PDF). This material is available free of charge via the Internet at http://pubs.acs.org.

JA020900A

(33) Allcock, H. R.; Lampe, F. W. *Contemporary Polymer Chemistry*, 2nd ed.; Prentice-Hall: New York, 1990; pp 508−509.

(34) Guilani, B.; Rasco, M. L.; Hermann, C. F. K.; Gibson, H. W. *J. Heterocycl. Chem.* **1990**, *27*, 1007−1009.